Inorganic Chemistry

pubs.acs.org/IC Article

Water-Soluble Rhenium Phosphine Complexes Incorporating the $Ph_2C(X)$ Motif (X = O^-, NH^-): Structural and Cytotoxicity Studies

Abdullah F. Alshamrani, Timothy J. Prior, Benjamin P. Burke, David P. Roberts, Stephen J. Archibald, Lee J. Higham, Graeme Stasiuk,* and Carl Redshaw*

Cite This: https://dx.doi.org/10.1021/acs.inorgchem.9b03239 Read Online

ACCESS | Metrics & More | Article Recommendations | Supporting Information

ABSTRACT: Reaction of $[ReOCl_3(PPh_3)_2]$ or $[ReO_2I(PPh_3)_2]$ with 2,2′-diphenylglycine ($dpgH_2$) in refluxing ethanol afforded the air-stable complex $[ReO(dpgH)(dpg)(PPh_3)]$ (**1**). Treatment of $[ReO(OEt)I_2(PPh_3)_2]$ with 1,2,3-triaza-7-phosphaadamantane (PTA) afforded the complex $[ReO(OEt)I_2(PTA)_2]$ (**2**). Reaction of $[ReOI_2(PTA)_3]$ with $dpgH_2$ led to the isolation of the complex $[Re(NCPh_2)I_2(PTA)_3]\cdot 0.5EtOH$ (**3**·0.5EtOH). A similar reaction but using $[ReOX_2(PTA)_3]$ (X = Cl, Br) resulted in the analogous halide complexes $[Re(NCPh_2)Cl_2(PTA)_3]\cdot 2EtOH$ (**4**·2EtOH) and $[Re(NCPh_2)(PTA)_3Br_2]\cdot 1.6EtOH$ (**5**·1.6EtOH). Using benzilic acid (2,2′-diphenylglycolic acid, benzH) with **2** afforded the complex $[ReO(benz)_2(PTA)][PTAH]\cdot EtOH$ (**6**·EtOH). The potential for the formation of complexes using radioisotopes with relatively short half-lives suitable for nuclear medicine applications by developing conditions for $[Re(NCPh_2)(dpg)I(PTA)_3]$ (**7**)$[ReO_4]^-$ in a 4 h time scale was investigated. A procedure for the technetium analog of complex $[Re(NCPh_2)I_2(PTA)_3]$ (**3**) from $^{99m}Tc[TcO_4]^-$ was then investigated. The molecular structures of **1**−**7** are reported; complexes **3**−**7** have been studied using in vitro cell assays (HeLa, HCT116, HT-29, and HEK 293) and were found to have IC_{50} values in the range of 29−1858 μM.

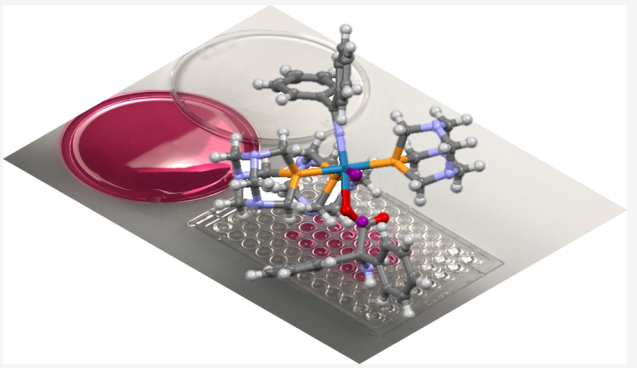

INTRODUCTION

The diagnosis and early treatment of diseases such as cancer and heart disease have benefited greatly from the availability of technetium-based imaging agents.[1] ^{99m}Tc is used as a γ-emitter in single-photon emission computed tomography (SPECT). Moreover, ^{99m}Tc has been used for diagnosis as an imaging agent because of the optimal 140-keV γ-ray emission, the 6 h half-life, lower tissue damage, and the availability of a convenient generator.[2−5] By contrast, rhenium has two isotopes that are β-emitters, namely, ^{186}Re and ^{188}Re, with half-lives ($t_{1/2}$) of 90 and 17 h, respectively, making them suitable as therapeutics in a theranostic pair with technetium.[6] Given the similarities between the chemistries of these two metals, any advances in the synthetic methodology to access one type of metal chelate can usually be applied to the other metal and vice versa.[2,7] Currently, much research effort is devoted to developing targeted agents, thereby ensuring any delivered radiation is localized.[3,8,9]

The use of chelates with added functional groups is a particularly promising avenue,[10] and with this in mind, we have initiated a program to investigate the use of amino acid derived chelates bound to rhenium. We note that data concerning the cellular uptake, toxicity, and localization of rhenium amino acid complexes are scant.[11] Moreover, the use of amino acid derived ligation at the rhenium core has been recognized as a potential method for modulating toxicity, localization, etc., in mammalian cells.[11,12] The use of amino acids has allowed for the development of many new chelate families, particularly where steric bulk is not a prerequisite for complex formation.[13,14] They can also act as bifunctional chelators, i.e., can attach to targeted biomolecules and bear coordination sites to the radionuclide that can direct the biodistribution of the radiotracer.[15−17] The use of simple carboxylic acids also allows for optical properties of metal complexes to be probed with a view to enhancing their bioapplication.[18,19] In other studies, we and others have found that the use of the acids $Ph_2C(X)CO_2H$ (X = OH, NH_2) can impart high crystallinity in products and be beneficial for characterization.[20−23] Thus, herein we report our initial studies on rhenium complexes bearing ligands derived from diphenylglycine (X = NH_2) and the related pro-ligand benzilic acid (X = OH).

Convenient entry points into high-oxidation-state rhenium chemistry are the phosphine complexes $[ReOCl_3(PPh_3)_2]$ and $[ReO_2I(PPh_3)_2]$; however, it must be noted that the low

Received: November 5, 2019

https://dx.doi.org/10.1021/acs.inorgchem.9b03239
Inorg. Chem. XXXX, XXX, XXX−XXX

biocompatibility, high molecular weight, and hydrophobicity of arylphosphines renders these complexes unsuitable for medical uses.[24] The challenge, therefore, is to replace PPh_3 with a more biocompatible and hydrophilic phosphine. 1,2,3-Triaza-7-phosphaadamantane (PTA) is a phosphine that is widely used as a water-soluble ligand and possesses an adamantane-like structure. Daigle et al. first prepared this phosphine in 1974, and because of its solubility and stability in water, it has been widely used in the fields of organometallic catalysis and coordination chemistry;[25,26] others have recently published on the coordination chemistry of PTA and outlined its medical and catalytic chemistry.[27−30] Thus, herein we have employed PTA to produce water-soluble rhenium complexes for facile biological evaluation. We also note that the rhenium oxo complexes can be isolated from [3 + 2] reactions involving diphenyl ketene.[31] The $dpgH_2$, benzH and complexes **1**−**7** prepared herein are shown below in Schemes 1 and 2.

Scheme 1. 2,2′-Diphenylglycine ($dpgH_2$) and Benzilic Acid (2,2′-Diphenylglycolic Acid, benzH)

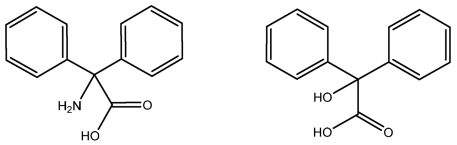

($dpgH_2$) (benzH)

Finally, given that the aim of this work is to develop new technetium-based imaging agents, we have conducted the preparation of a water-soluble $dpgH_2$-derived rhenium complex from $(NH_4)[ReO_4]$ in 4 h and have investigated this synthetic methodology with $[^{99m}Tc]TcO_4^-$.

EXPERIMENTAL SECTION

General Information. All manipulations were carried out under an atmosphere of dry nitrogen using conventional Schlenk and cannula techniques or in a conventional nitrogen-filled glovebox. Hexane and ethanol were dried over sodium prior to use. Dichloromethane was refluxed over calcium hydride. Diethyl ether was dried over sodium benzophenone. All solvents were distilled and degassed prior to use. IR spectra (nujol mulls, KBr windows) were recorded on a Nicolet Avatar 360 FT IR spectrometer; ^1H NMR spectra were recorded at room temperature on a Varian VXR 400 S spectrometer at 400 MHz or a Gemini 300 NMR spectrometer or a Bruker Advance DPX-300 spectrometer at 300 MHz. The ^1H NMR spectra were calibrated against the residual protio impurity of the deuterated solvent. Elemental analyses were performed by the elemental analysis service at the London Metropolitan University and the Department of Chemistry and Biochemistry at the University of Hull.

The precursors $[ReOCl_3(PPh_3)_2]$, $[ReOBr_3(PPh_3)_2]$, $[ReO_2I(PPh_3)_2]$, $[ReO(OEt)I_2(PPh_3)_2]$, and $[ReOCl_2(PTA)_3]$ were prepared by the literature methods; $[ReOX_2(PTA)_3]$ (X = Br, I) was prepared following the method used for $[ReOCl_2(PTA)_3]$.[24,32−34] All other chemicals were purchased from Sigma-Aldrich.

*Synthesis of [ReO(dpgH)(dpg)(PPh$_3$)] (**1**).* To $[ReOCl_3(PPh_3)_2]$ (0.50 g, 0.60 mmol) and 2,2′-diphenylglycine (0.27 g, 1.20 mmol) was added dry ethanol (20 mL). After the mixture was refluxed for 4 h, volatiles were removed in vacuum and the residue was extracted into CH_2Cl_2 (20 mL). Addition of a layer of Et_2O (20 mL) afforded, on prolonged standing, green prisms of **1**. Yield: 0.40 g (74%). Elemental anal. calcd for $C_{46}H_{38}N_2O_5PRe$: C, 60.26%; H, 4.14%; N, 3.05%. Found: C, 59.93%; H, 4.00%; N 3.02%. ^1H NMR ($CDCl_3$) δ: 11.24 (s, 1H, NH), 7.13−7.51 (m, 21H, $H_{arom}PPh_3/CPh_2$), 6.98 (d, J = 8.2 Hz, 6H, $H_{arom}PPh_3$), 6.67 (d, J = 11.4 Hz, 8H, H_{arom} CPh_2), 5.92 (d, J = 11.4 Hz, 2H, NH_2). ^{31}P NMR ($CDCl_3$) δ: 5.3 (s). IR (KBr): 3303 (w), 3258 (w), 1584 (m), 1569 (m), 1092 (s), 998 (s), 980 (s), 955 (s), 936 (s), 908 (s) cm^{-1}. MALDI-MS m/z: 917.21 $[M + H^+]$.

*Synthesis of [ReO(dpgH)(dpg)(PPh$_3$)] (**1**) from [ReO$_2$I(PPh$_3$)$_2$].* As above, but using $[ReO_2I(PPh_3)_2]$ (0.50 g, 0.57 mmol) and 2,2′-diphenylglycine (0.26 g, 1.14 mmol), afforded **1** as green prisms. Yield: 0.30 g (57%). Elemental anal. calcd for $C_{46}H_{38}N_2O_5PRe$: C, 60.26%; H, 4.14%; N, 3.05%. Found: C, 60.32%; H, 3.89%; N, 3.07%. ^1H NMR ($CDCl_3$) δ: 11.24 (s, 1H, NH), 6.91−7.72 (m, 21H, $H_{arom}PPh_3/CPh_2$), 6.66 (d, J = 11.5, 14H, $H_{arom}PPh_3/CPh_2$), 5.92 (d, J = 11.5, 2H, NH_2). ^{31}P NMR ($CDCl_3$) δ: 5.3 (s). IR (KBr): 3301 (w), 3256 (w), 1584 (w), 1569 (w), 1092 (s), 998 (s), 979 (m), 955 (m), 936 (m), 908 (m) cm^{-1}. MALDI-MS m/z: 917.21 $[M + H^+]$.

*Synthesis of [ReO(OEt)I$_2$(PTA)$_2$] (**2**).* At room temperature, 1,3,5-triaza-7-phosphaadamantane (0.51 g, 3.27 mmol) was dissolved in the minimum volume of dichloromethane (∼30 mL), and the solution was added to a conical flask containing a suspension of $[ReO(OEt)I_2(PPh_3)_2]$ (1.00 g, 1.09 mmol) in dichloromethane (20 mL), which caused a color change from light khaki to yellow-orange. The reaction mixture was stirred for 1 h, and then the volatiles were removed under vacuum. Ethanol (5 mL) was added, and slow evaporation of the solvent at room temperature afforded a yellow-orange solid, which was collected and washed with EtOH (10 mL) and Et_2O (10 mL). Orange crystals of **2** suitable for X-ray crystallography were obtained by recrystallization from CH_2Cl_2/EtOH. Yield: 0.81 g (92%). Elemental anal. calcd for $C_{14}H_{29}I_2N_6O_2P_2Re$: C, 20.60%; H, 3.55%; N, 10.30%. Found: C, 21.01%; H, 3.95%; N, 10.64%. ^1H NMR ($CDCl_3$) δ: 4.48−4.74 (m, 2H, CH_2), 4.03−4.35 (m, 12H, N−CH_2−N), 3.87 (d, J = 9.2 Hz, 12H, P-CH_2), 1.58 (s, 3H, CH_3). ^{31}P NMR ($CDCl_3$) δ: −4.8 (s); in (D_2O) δ: −2.2 (s). IR (KBr): 1281 (m), 1040 (m), 1013 (s), 969 (s), 945 (s), 902 (s) cm^{-1}. MALDI-MS m/z: 816.95 $[M + H^+]$.

*Synthesis of [Re(NCPh$_2$)I$_2$(PTA)$_3$]·0.5EtOH (**3**·0.5EtOH).* To $[ReOI_2(PTA)_3]$ (0.50 g, 0.53 mmol) and $dpgH_2$ (0.24 g, 1.07 mmol) was added dry ethanol (20 mL). After the mixture was refluxed for 4 h, the solution was filtered, and on prolonged standing (2 to 3 days) at ambient temperature, green crystals of **3** formed. Yield: 0.40 g (68%). Elemental anal. calcd for $C_{64}H_{88}I_4N_{20}P_6Re_2$·0.5EtOH: C, 34.57%; H, 4.41%; N, 12.60%. Found: C, 34.90%; H, 4.79%; N, 12.72%. ^1H NMR (C_6D_6) δ: 7.05−7.29 (m, 10H, $H_{arom}CPh_2$), 3.85−4.08 (m, 18H, N−CH_2−N), 3.66 (d, J = 41.6 Hz, 18H, P-CH_2). ^{31}P NMR (C_6D_6) δ: −104.9 (t, J = 11.3 Hz), −120.9 (d, J = 12.5 Hz); in ($CDCl_3$) δ: −104.2 (t, J = 12.5 Hz), −118.7 (d, J = 12.5 Hz); in (D_2O) δ: −107.3 (t, J = 11.3 Hz), −123.3 (d, J = 12.5 Hz). IR (KBr): 1592 (w), 1416 (m), 1313 (m), 1276 (s), 1241 (s), 1041 (m), 1015 (s), 969 (s), 946 (s) cm^{-1}. ES-MS m/z: 1092 $[M + H^+]$.

*Synthesis of [Re(NCPh$_2$)Cl$_2$(PTA)$_3$]·2EtOH (**4**·2EtOH).* To $[ReOCl_2(PTA)_3]$ (0.50 g, 0.68 mmol) and $dpgH_2$ (0.27 g, 1.10 mmol) was added dry ethanol (20 mL). After the mixture was refluxed for 4 h, the solution was filtered, and on prolonged standing (2 to 3 days) at ambient temperature, green crystals of **4** formed. Yield: 0.40 g (67%). Elemental anal. calcd for $C_{31}H_{46}Cl_2N_{10}P_3Re$ (sample dried in-vacuum −2EtOH): C, 40.93%; H, 5.06%; N, 15.40%. Found: C, 40.52%; H, 4.95%; N, 15.01%. ^1H NMR (C_6D_6) δ: 7.06−7.29 (m, 10H, $H_{arom}CPh_2$), 3.55−3.63 (m, 18H, N−CH_2−N), 3.19 (d, J = 8.7 Hz, 18H, P-CH_2). ^{31}P NMR (C_6D_6) δ: −82.0 (t, J = 10.0 Hz), −94.9 (d, J = 10.0 Hz); in ($CDCl_3$) δ: −81.2 (t, J = 10.0 Hz), −94.2 (d, J = 10.0 Hz); in (D_2O) δ: −77.4 (t, J = 10.0 Hz), −91.6 (d, J = 7.5 Hz). IR (KBr): 1598 (w), 1462 (s), 1315 (w), 1281 (w), 1242 (w), 1040 (w), 1015 (m), 972 (m), 947 (m) cm^{-1}.MALDI-MS m/z: 909.20 $[M + H^+]$.

*Synthesis of [Re(NCPh$_2$)Br$_2$(PTA)$_3$]·1.6EtOH (**5**·1.6EtOH).* To $[ReOBr_2(PTA)_3]$ (0.50 g, 0.60 mmol) and $dpgH_2$ (0.27 g, 1.20 mmol) was added dry ethanol (20 mL). After the mixture was refluxed for 4 h, the solution was filtered, and on prolonged standing (2 to 3 days) at ambient temperature, green crystals of **5** formed. Yield: 0.35 g (58%). Elemental anal. calcd for $C_{31}H_{46}Br_2N_{10}P_3Re$·0.5EtOH (sample dried in-vacuum, −1.1EtOH): C, 37.64%; H, 4.80%; N, 13.72%. Found: C, 37.83%; H, 5.18%; N, 13.26%. ^1H NMR (DMSO−D_6) δ: 7.53 (t, J = 7.8 Hz, 6H, $H_{arom}CPh_2$), 6.94−7.11 (m,

https://dx.doi.org/10.1021/acs.inorgchem.9b03239
Inorg. Chem. XXXX, XXX, XXX−XXX

Scheme 2. Complexes 1−7 Prepared Herein

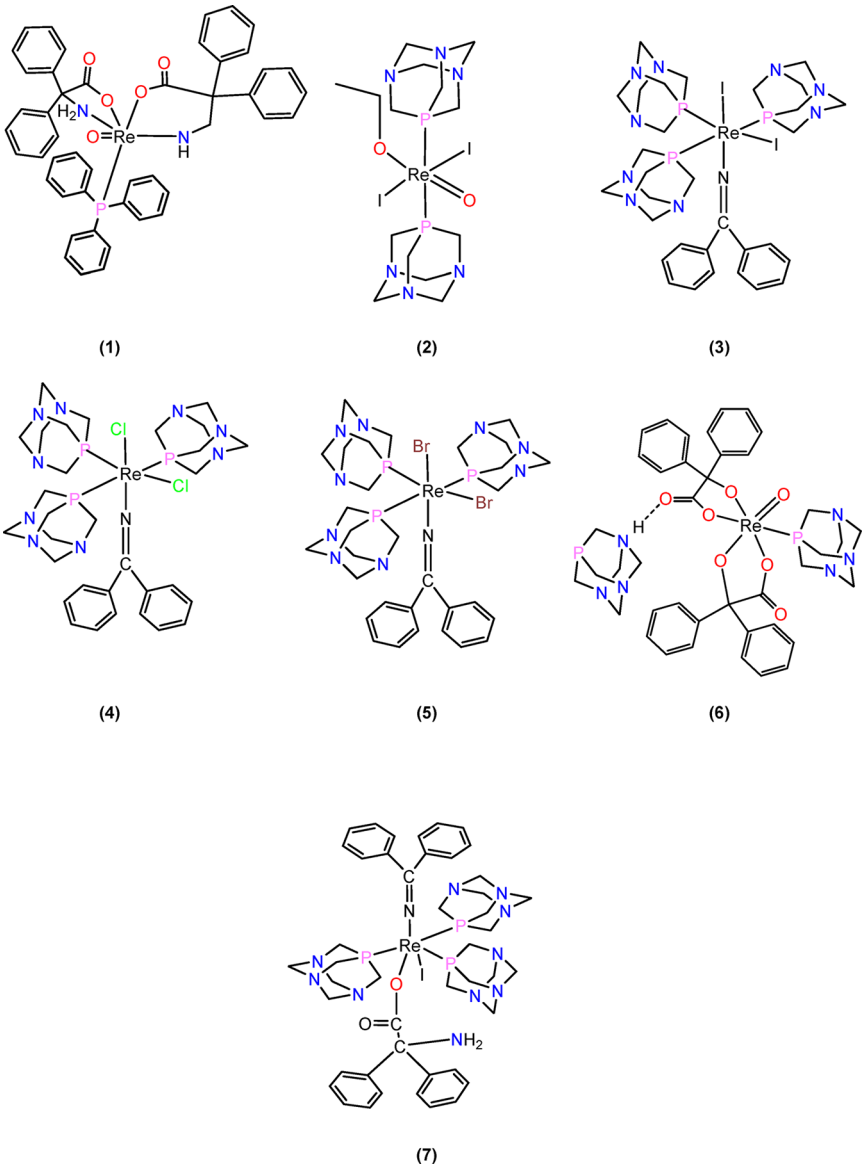

4H, $H_{arom}CPh_2$), 3.91−4.39 (m, 18H, N−CH_2−N), 3.73 (d, J = 9.6 Hz, 18H, P-CH_2). ^{31}P NMR (DMSO−D_6) δ: −87.5 (t, J = 10.0 Hz), −103.6 (d, J = 10.0 Hz); in ($CDCl_3$) δ: −89.4 (t, J = 10.0 Hz), −103.3 (d, J = 10.0 Hz); in (D_2O) δ: −70.8(m), −82.2 (d, J = 5 Hz). IR (KBr): 1459 (s), 1376 (s), 1281 (m), 1277 (m), 1239 (m), 1094 (s), 1040 (m), 1011 (s), 969 (s), 945 (s) cm^{-1}. MALDI-MS m/z: 840.68 [M − PTA].

*Synthesis of [ReO(benz)$_2$(PTA)][PTAH]·EtOH (**6**·EtOH).* To [ReO(OEt)I_2(PTA)$_2$] (0.61 g, 0.74 mmol) and benzilic acid (0.34 g, 1.48 mmol) was added dry ethanol (20 mL). After the mixture was refluxed for 4 h, the solution was allowed to cool to room temperature, whereupon purple crystals of **6**·EtOH formed. Yield: 0.50 g (68%). Elemental anal. calcd for $C_{82}H_{96}N_{12}O_{15}P_4Re_2$: C, 49.47%; H, 4.87%; N, 8.47%. Found: C, 49.35%; H, 4.60%; N, 8.65%. ^{1}H NMR (C_6D_6) δ: 7.24−7.96 (m, 20H, $H_{arom}CPh_4$), 3.22−3.29 (m, 12H, N−CH_2−N), 2.91 (d, J = 7.8 Hz, 12H, P-CH_2). ^{31}P NMR (C_6D_6) δ: −90.4 (s), −94.5 (s); in (D_2O) δ: −88.5 (s), −91.6 (s). IR (KBr): 1656 (s), 1631 (s), 1025 (s), 1011 (m), 981 (w), 969 (s), 945 (s), 923 (w) cm^{-1}. MALDI-MS m/z: 971.24 [M + H$^+$].

*Synthesis of [Re(NCPh$_2$)(dpg)I(PTA)$_3$]·2C_6D_6 (**7**·2C_6D_6).* Ammonium perrhenate (1.09 g, 4.10 mmol) and triphenylphosphine (5.00 g, 19.0 mmol) were stirred in ethanol (30 mL). Hydroiodic acid (56%, 5 mL) was then added carefully, and the brown mixture was heated under reflux for 15 min. The obtained olive-green solid was filtered off and washed with ethanol (25 mL) and diethyl ether (25 mL), with no further drying. This compound was then added to the solvent mixture (1:25) (water/acetone), which was stirred in an ice bath for 30 min. A violet compound [$ReO_2I(PPh_3)_2$] precipitated which was then filtered off and dried in vacuum. 1,3,5-Triaza-7-phosphaadamantane (2.17 g, 13.8 mmol) was dissolved in a minimum volume of dichloromethane, and the solution was then mixed (at room temperature) with the preprepared [$ReO_2I(PPh_3)_2$] (2.00 g, 2.30 mmol) dissolved in dichloromethane (30 mL); the color changed from dark brown to pale brown. The reaction mixture was stirred for 40−50 min, following which the volume of the solution was reduced in under vacuum to remove any volatiles. Ethanol (5 mL) was then added, and after 5 min, the remaining solvent was removed using a rotary evaporator. The obtained product was then washed with ethanol to give a yellow-orange solid [$ReO_2I(PTA)_3$]. Finally, [$ReO_2I(PTA)_3$] (2.00 g, 2.44 mmol) and $dpgH_2$ (1.11 g, 4.88 mmol) were mixed in ethanol (20 mL). The reaction was then stirred at 100 °C under reflux for 90 min to produce a green solution. This green solution was filtered, and the solvent was then removed via rotary evaporation to produce a fine green solid of complex 7. Yield: 1.80 g (62%). Green crystals suitable for X-ray analysis were obtained by recrystallization of the product [$Re(NCPh_2)(dpg)I(PTA)_3$] (7) in benzene. Elemental

https://dx.doi.org/10.1021/acs.inorgchem.9b03239
Inorg. Chem. XXXX, XXX, XXX−XXX

Table 1. Crystallographic Data for Complexes 1−7

	1	2	3	4	5	6	7
empirical formula	$C_{46}H_{38}N_2O_5PRe$	$C_{14}H_{29}I_2N_6O_2P_2Re$	$C_{64}H_{88}I_4N_{20}OP_6Re_2\cdot 0.5EtOH$	$C_{31}H_{46}Cl_2N_{10}P_3Re\cdot 2EtOH$	$C_{31}H_{46}Br_2N_{10}P_3Re\cdot 1.6EtOH$	$C_{82}H_{96}N_{12}O_{15}P_4Re_2\cdot EtOH$	$C_{54.90}H_{68.20}I_{1.15}N_{10.15}O_{1.70}P_3Re\cdot 2C_6D_6$
formula weight	915.95	815.37	2219.36	908.79	997.71	1985.98	1332.34
temperature	100(2) K	100(2) K	100(2) K	150(2) K	150(2) K	150(2) K	150(2) K
wavelength	0.71075 Å	0.71073 Å	0.71075 Å	0.71073 Å	0.71073 Å	0.71075 Å	0.71073 Å
crystal system	triclinic	monoclinic	triclinic	triclinic	triclinic	triclinic	monoclinic
space group	$P\bar{1}$	$P2_1/n$	$P\bar{1}$	$P\bar{1}$	$P\bar{1}$	$P\bar{1}$	$P2_1/n$
unit cell dimensions							
a [Å]	13.2798(2)	25.1208(13)	10.22760(10)	10.3595(14)	10.1478(7)	9.5325(2)	11.7130(4)
b [Å]	23.0757(5)	6.8178(4)	13.56420(10)	11.1139(16)	13.6036(9)	10.6561(2)	17.6413(6)
c [Å]	26.1765(6)	26.2202(15)	15.3839(2)	18.707(4)	15.4971(10)	20.9031(4)	27.1727(8)
α [°]	108.600 (2)	90	84.3800(10)	100.944(14)	83.257(5)	78.781(2)	90
β [°]	92.629(2)	99.070(4)	81.5650(10)	98.250(13)	80.541(5)	87.0180(10)	91.979(3)
γ [°]	91.153(2)	90	79.7640(10)	102.248(11)	79.193(5)	4.910(2)	90
volume [Å^3]	7589.4(3)	4434.5(4)	2071.84(4)	2028.2(4)	2064.5(2)	2010.93(4)	5611.4(3)
Z	8	8	1	2	2	1	4
density [Mg/m^3]	1.603	2.443	1.779	1.488	1.605	1.640	1.577
μ(Mo−Kα) [mm^{-1}]	3.296	8.432	4.575	3.280	2.029	3.161	2.934
F(000)	3664	3056	1072	912	984	1002	2672
crystal size [mm^3]	0.280 × 0.150 × 0.015	0.320 × 0.110 × 0.080	0.15 × 0.05 × 0.04	0.45 × 0.32 × 0.14	0.380 × 0.170 × 0.070	0.120 × 0.110 × 0.100	0.350 × 0.170 × 0.046
theta range for data collection	2.336−27.486°	1.573−25.681°	2.108−27.483°	1.926−29.777°	2.065−25.027°	2.427−27.484°	1.893−29.294°
reflections collected	78981	18045	57568	31040	14392	45855	40245
independent reflections	32137 [R(int) = 0.0444]	8310 [R(int) = 0.0469]	9493 [R(int) = 0.0417]	10839 [R(int) = 0.0370]	7207 [R(int) = 0.0745]	9203 [R(int) = 0.0334]	15019 [R(int) = 0.1115]
completeness to theta = 25.242°	96.0%	98.7%	99.9%	99.3%	99.1%	99.9%	99.2%
data/restraints/parameters	32137/1632/2020	8310/478/487	9493/2/436	10839/465/424	7207/0/424	9203/20/546	15019/79/638
goodness-of-fit on F^2	1.118	0.695	1.096	0.946	0.938	1.06	0.855
$\Delta\rho_{max}$; $\Delta\rho_{min}$ [eÅ^{-3}]	0.870; −1.314	1.249; −0.893	1.566; −2.250	1.557; −1.006	2.635; −1.864	1.530; −0.548	1.434; −3.886
R_1 [$I > 2\sigma(I)$]	0.0549	0.0234	0.0363	0.0245	0.0470	0.0190	0.0541
wR_2 (all data)	0.1109	0.0473	0.0856	0.0576	0.1138	0.0464	0.1397

https://dx.doi.org/10.1021/acs.inorgchem.9b03239
Inorg. Chem. XXXX, XXX, XXX−XXX

anal. calcd for $C_{45}H_{58}I_1N_{11}P_3Re$: C, 45.34%; H, 4.86%; N, 12.93%. Found: C, 45.12%; H, 5.12%; N 12.72%. ^{1}H NMR (C_6D_6) δ: 7.64 (d, J = 8.3 Hz, 4H, $H_{arom}CPh_2$), 6.82−7.34 (m, 6H, $H_{arom}CPh_2$), 3.55−4.34 (m, 32H, CH_2(PTA)), 3.17−3.40 (m, 2 H, NH_2). ^{31}P NMR (C_6D_6) δ: −4.7 (s), −102.3 (s); in ($CDCl_3$) δ: −4.8 (s), −98.2 (s); in (D_2O) δ: −2.2 (s), −95.3 (s). IR (KBr): 3409 (w), 1633 (m), 1035 (w), 1012 (s), 968 (m), 945 (m) cm^{-1}. MALDI-MS m/z: 1191.80 [M]$^+$, 1175.85 [M$^+$ − NH_2].

Synthesis of [^{99m}Tc][Tc(NCPh$_2$)I$_2$(PTA)$_3$]. [^{99m}Tc]TcO_4^- was eluted in saline from an Ultra Technekow FM ^{99}Mo/^{99m}Tc generator (Curium, U.K.), and 100 μL (∼200 MBq, in saline) was added to a 2 mL glass vial containing a mixture of 900 μL of dimethylformamide (DMF), triphenylphosphine (66.5 mg, 0.255 mmol), and hydroiodic acid (66.5 μL, 0.883 mmol). The vial was heated at 137 °C for 30 min. After the vial was allowed to cool, a solution of 1,3,5-triaza-7-phosphaadmantane (3.7 mg, 0.0235 mmol) in DMF (100 μL) was added to the reaction mixture, and the mixture was stirred for 40 min at 99 °C. Finally, a solution of 2,2′-diphenylglycine (0.17 mg, 0.00074 mmol) in DMF (10 μL) was added to the reaction mixture, and the mixture was stirred at 137 °C for 2 h. Quality control analysis was carried out by HPLC or radio-TLC. Radio-TLC experiments were carried out on aluminum-backed silica TLC plates with saline as the mobile phase. Detection was performed using a Scan-RAM Radio TLC detector. [^{99m}Tc]TcO_4^- RF = 0.967; [^{99m}Tc] [$TcO_2I(PPh_3)_2$] RF = 0.04; and [^{99m}Tc][$TcOI_2(PTA)_3$] RF = 0.087.

HPLC Conditions. HPLC analysis was performed on an Agilent 1100 Series system equipped with a diode array UV (detection at 254 nm) and LabLogic NaI crystal gamma detectors controlled by Laura software.

The analytical HPLC was performed on a Gemini 5 μm C18 110 Å LC column (150 × 4.6 mm, Phenomenex) at a flow rate of 1 mL min^{-1}, with a mobile phase consisting of methanol with 0.1% TFA (solvent A) and water with 0.1% TFA (solvent B). Gradient 1 [time/min](solvent A/solvent B): [0−2](50:50), [2−17](95:5), [17−22](95:5), [22−26](50:50). The HPLC sample was prepared by taking 10 μL of sample dissolved in 90 μL of methanol. Semipreparative HPLC was carried out on a Luna 5 μm C18(2) 100 Å LC column (250 × 10 mm; Phenomenex) and a Pursuit 200 Å C18 10 × 250 mm, 10 μm, HPLC column (Agilent) at a flow rate of 5 mL min^{-1}, with a mobile phase consisting of methanol with 0.1% TFA (solvent A) and water with 0.1% TFA (solvent B). Semipreparative gradient [time/min](solvent A/solvent B): [0−2](95:5), [2−22](95:5−50:50), [0−2](95:5), [2−22](95:5−50:50). Prior to the HPLC purification, the reaction mixtures were passed through C-18 cartridges to trap unreacted [^{99m}Tc]TcO_4^-.

X-ray Crystallography. X-ray diffraction data from single crystals of **3**·0.5EtOH and **6**·EtOH were collected at the EPSRC crystallography service in Southampton, U.K. For the other samples, full sets of X-ray diffraction intensity data were collected in series of ω-scans using a Stoe IPDS2 image plate diffractometer operating with Mo Kα radiation at 150(2) K. A multiscan method was applied for the absorption corrections of the collected data.[35]

The structures were solved using dual-space methods within SHELXT and full-matrix least-squares refinement was carried out within SHELXL-2018 via the WinGX program interface.[36,37] All non-hydrogen positions were located in the direct and difference Fourier maps and refined using anisotropic displacement parameters. Crystal structure data for the compounds reported here are summarized in Table 1.

Cytotoxicity. MTS assay was used to calculate the percentage of viable cells in the culture media. This assay depends on the transformation of a tetrazolium salt into formazan in viable cells by mitochondrial dehydrogenase enzyme activity. There is a positive correlation between the amount of formazan and the number of viable cells in the culture media. HeLa, HCT116, HT-29, and HEK 293 cells were seeded in 96 flat-bottomed microliter tissue culture plates with 20 000 cells per well in 200 μL media of McCoy's and Dulbecco's Modified Eagle's Medium (DMEM). In order to attach the cells to the well base in the microliter plates, the plates were incubated overnight in a 5% CO_2 incubator at 37 °C. After 24 h, the media was removed from the wells and 100 μL of the compound in the media was added. Various concentrations of compounds in the range of 6.25 mM to 6.25 nM were tested. After 24 h of incubation, the contents of the wells were removed using a multipipette, and then 180 μL of sterilized PBS was added followed by the addition of 20 μL of MTS reagent (Promega, U.K.). Plates were then returned to the incubator for 4 h. Color intensity (absorbance) of the treated wells was measured at 490 nm using a Synergy HT microplate reader. The percentages of the cell viability of the treated cells were calculated based on positive and negative control where they represent 100% and 0% viable cells, respectively. IC_{50} values were calculated using GraphPad Prism software.

RESULTS AND DISCUSSION

Use of 2,2′-Diphenylglycine. A convenient entry point into much rhenium(V) oxo chemistry is the readily available [$ReOCl_3(PPh_3)_2$].[38] Reaction of this complex with two equivalents of $dpgH_2$ in refluxing ethanol afforded, following workup, the green complex [ReO(dpgH)(dpg)(PPh_3)] (**1**) in moderate-to-good yield (≤74%). The IR spectrum contained a strong band at 955 cm^{-1} assigned to $\nu_{Re=O}$ along with strong Re−P stretches at 1092 cm^{-1} and ν_{N-H} at 3303 cm^{-1}. The ^{31}P NMR spectrum displayed a singlet at δ 5.3 ppm for the PPh_3 ligand. Single crystals suitable for an X-ray crystal structure determination were grown by diffusing diethyl ether into a saturated dichloromethane solution at ambient temperature. The crystal structure of **1** is rather complex because there are four chemically equivalent, but symmetry-independent molecules in the asymmetric unit. Each of these four molecules features the same binding of the ligands, but these molecules have phenyl rings in different orientations which renders them symmetry independent. Rather than describe the four related molecules in words, the geometry about the metal for one of these is reported and displayed in Figure 1 (the full asymmetric

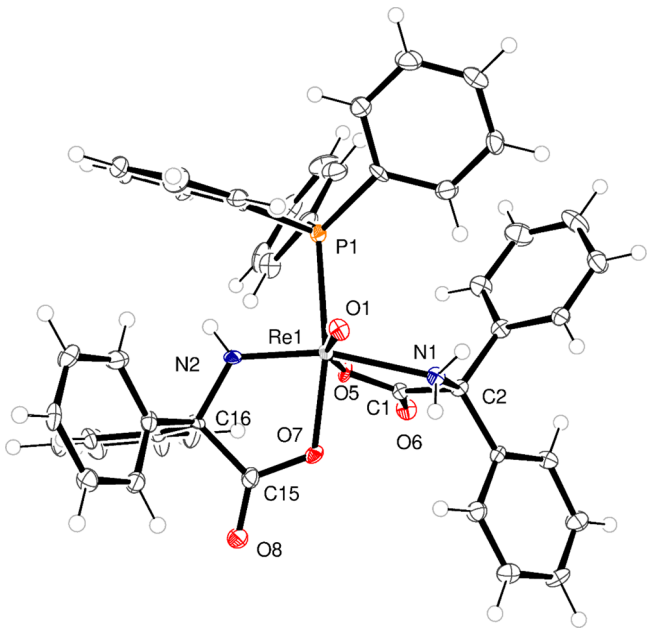

Figure 1. Molecular structure of one metal ion in [ReO(dpgH)(dpg)(PPh_3)] (**1**). Selected bond lengths (Å) and angles (deg): Re(1)−O(1) 1.705(4), Re(1)−O(5) 2.064(4), Re(1)−O(7) 2.025(3), Re(1)−N(1) 2.250(5), Re(1)−N(2) 1.889(5), Re(1)−P(1) 2.4487(13); O(5)−Re(1)−N(1) 73.85(15), O(1)−Re(1)−O(7) 104.88(15), N(2)−Re(1)−O(7) 80.47(16), O(5)−Re(1)−P(1) 88.69(10).

https://dx.doi.org/10.1021/acs.inorgchem.9b03239
Inorg. Chem. XXXX, XXX, XXX−XXX

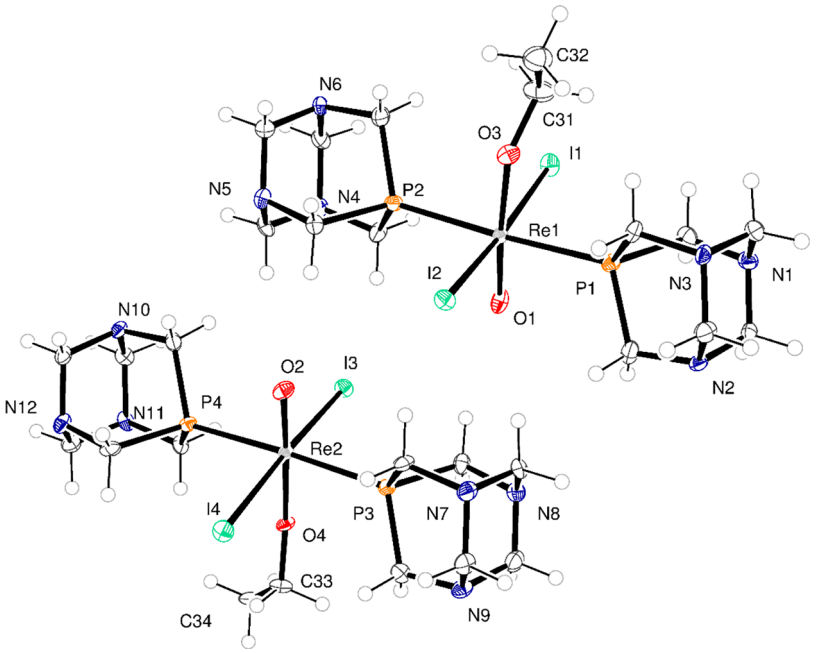

Figure 2. Molecular structure of $[ReO(OEt)I_2(PTA)_2]$ (**2**). Selected bond lengths (Å) and angles (deg): Re(1)−O(1) 1.706(5), Re(1)−O(3) 1.906(5), Re(1)−I(1) 2.8117(5), Re(1)−I(2) 2.7450(5), Re(1)−P(1) 2.4673(17), Re(1)−P(2) 2.4523(17); O(1)−Re(1)−O(3) 172.6(2), P(2)−Re(1)−P(1) 176.27(6), O(1)−Re(1)−I(2) 95.59(16), C(31)−O(3)−Re(1) 146.9(4), O(3)−C(31)−C(32) 111.9(6). Re(2)−O(2) 1.705(5), Re(2)−O(4) 1.906(5), Re(2)−I(3) 2.7519(5), Re(2)−I(4) 2.8080(5), Re(2)−P(3) 2.4555(17), Re(2)−P(4) 2.4631(17); O(2)−Re(2)−O(4) 174.3(2), P(3)−Re(2)−P(4) 176.24(6), O(2)−Re(2)−I(3) 94.42(15), C(33)−O(4)−Re(2) 152.0(4), O(4)−C(33)−C(34) 111.2(5).

unit and full details of bond lengths about each metal center are in the SI.) The metal ion adopts a distorted octahedral geometry where the main distortion occurs as a result of binding through COO^- and NH^- of the two diphenylglycine-derived ligands. One of these (dpgH) is only deprotonated at the acid, but is bound through the NH_2 (Re(1)−N(1) 2.250(5) Å). The second is twice-deprotonated, i.e., dpg, once at the carboxylic acid and once at the amine, and it binds through COO^- and NH^-. Accordingly, the two Re−N bond lengths are very different (Re(1)−N(2) 1.889(5) Å).

It proved possible to obtain **1** by use of a similar reaction but employing $[ReO_2I(PPh_3)_2]$ as the rhenium source.

With a view to conducting biological assays, we decided to employ the water soluble phosphine 1,2,3-triaza-7-phosphaadamantane (PTA). Treatment of $[ReO(OEt)I_2(PPh_3)_2]$ with three equivalents of PTA in dichloromethane/ethanol afforded, after workup, the complex $[ReO(OEt)I_2(PTA)_2]$ (**2**) in high yield. The IR spectrum was dominated by the signals of $\nu_{Re=O}$ at 945 and 902 cm^{-1} for $\nu_{(O-CH2)}$. Also, the IR spectrum contained strong bands of coordinated PTA ligand at 969 and 1013 cm^{-1}. The ^1H NMR spectrum exhibited methylene protons for PTA between 4.03 and 4.74 ppm, while there were no signals displayed for the aromatic groups related to a PPh_3 ligand. The ^{31}P NMR spectrum showed a singlet at −4.8 ppm, suggesting the presence of two equivalent PTA ligands.

Single crystals suitable for a structure determination were grown via diffusion of dichloromethane/ethanol at ambient temperature. Structure determination for the crystal at 150 K was routine, and this demonstrated that **2** crystallized with two chemically identical molecules in the asymmetric unit ($Z = 2$) in space group $P2_1/n$.

The molecular structure is shown in Figure 2, with bond lengths and angles given in the caption. Each rhenium center adopts a distorted octahedral geometry with one bulky PTA ligand *trans* to the one other PTA. An ethoxide ligand is positioned *trans* to the oxo group.

The two independent complexes in the asymmetric unit are related by pseudo-translational symmetry. Upon warming of the crystal, the structure simplifies and the pseudo-translation becomes a strict symmetry element. The structure at 298 K crystallizes in the space group $C2/c$ with a single Re complex in the asymmetric unit ($Z = 4$) (Figure S3). There is small-scale disorder of the position of the ethoxide alkyl chain in this structure, which suggests that the presence of two independent complexes at low temperature is a result of ordering of the alkyl chains.

The reaction of $[ReOI_2(PTA)_3]$ with two equivalents of $dpgH_2$ in ethanol afforded, after workup, the complex $[Re(NCPh_2)(PTA)_3I_2]0.5EtOH$ (**3**·0.5EtOH). The infrared spectrum of **3** exhibited the signals of PTA ligands at 946, 969, and 1015 cm^{-1}, together with a weak band for $\nu_{N=C}$ at 1592 cm^{-1}. Also, in the IR spectrum, symmetric ν_{P-CH2} was found at 1313 cm^{-1}, while ν_{N-CH2} and ν_{N-C-N} were observed at 1276 and 1241 cm^{-1}, respectively. The ^1H NMR spectrum displayed signals for methylene protons of PTA between 3.66 and 4.08 ppm as well as aromatics between 7.05 and 7.29 ppm. The ^{31}P NMR spectrum (C_6D_6) exhibited (similar shifts were noted in $CDCl_3$, see the Experimental Section) a triplet and doublet at δ −104.9 and −120.9 ppm; these shifts (and those of **4** and **5**) are somewhat downfield of those reported for the complex $[ReNCl_2(PTA)_3]$ (−78.2 and −74.5 ppm in $CDCl_3$).[24] This data is consistent with the presence of two equivalent and one other PTA ligands. In order to assess the stability of complex **3**, a sample of **3** was dissolved in D_2O and monitored by ^{31}P NMR spectroscopy. The spectrum showed the peak of one PTA at −107.3 ppm and two PTA ligands *trans* to each other at −123.3 ppm. The two signals look similar to the triplet-

https://dx.doi.org/10.1021/acs.inorgchem.9b03239
Inorg. Chem. XXXX, XXX, XXX−XXX

doublet pattern of **3** in C_6D_6 (−104.9 and −120.9 ppm). Complex **3** was isolated as single crystals from EtOH, and the crystal structure was determined by X-ray diffraction. The molecular structure is shown in Figure 3 (for an alternative view see Figure S4), with selected bond lengths and angles given in the caption. The rhenium center adopts a distorted octahedral geometry in which the phosphine Re(1)−P(1) binds *trans* to the Re(1)−P(3). The distortion occurs as a result of the bulky nature of all the ligands present.

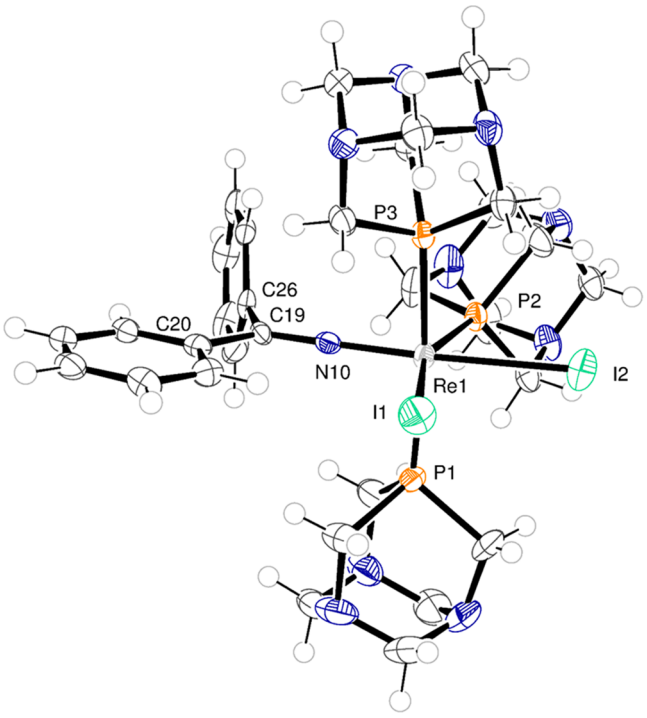

Figure 3. Molecular structure of **3**·0.5EtOH (unbound ethanol not shown). Selected bond lengths (Å) and angles (deg): Re(1)−I(1) 2.7939(4), Re(1)−I(2) 2.8652(4), Re(1)−P(1) 2.3929(12), Re(1)−P(2) 2.3911(11), Re(1)−P(3) 2.4004(12), N(10)−Re(1) 1.817(4), N(10)−C(19) 1.279(6); I(1)−Re(1)−I(2) 82.391(11), P(2)−Re(1)−P(1) 94.14(4), Re(1)−N(10)−C(19) 179.3(3).

In accordance with the structure of **3**, the Re(1)−P(1) and Re(1)−P(3) bonds found in the *trans* positions each display longer distances of 2.3929(12) and 2.4004(12) Å. The Re(1)−I(2) bond lengthening of 2.8652(4) Å can be ascribed to *trans* influence exerted by the Re(1)−N(10) that itself has a bond length of 1.817(4) Å. We have noted the loss of CO_2 from $dpgH_2$ during complexation in previous studies,[39,40] while a search of the CSD for $MNCPh_2$ or $MNCHPh_2$ type motifs revealed 19 hits.[39,41,42]

A similar reaction but using $[ReOCl_2(PTA)_3]$ and $[ReOBr_2(PTA)_3]$ also resulted after workup in the isolation of a green complex of formula $[Re(NCPh_2)(PTA)_3Cl_2]\cdot 2EtOH$ (**4**·2EtOH) and $[Re(NCPh_2)(PTA)_3Br_2]\cdot 1.6EtOH$ (**5**·1.6EtOH), respectively. However, a single-crystal X-ray diffraction study revealed that although the geometry at the metal is essentially the same as in **3**, there are different amounts of solvent present. The molecular structures for complexes **4**·2EtOH and **5**·1.6EtOH are shown in Figure 4 (for alternative views see Figures S5 and S6), with selected bond lengths and angles given in the caption.

Use of Benzilic Acid. The reaction of $[ReO(OEt)I_2(PTA)_2]$ (**2**) with two equivalents of benzilic acid in ethanol afforded, after workup, the complex $[ReO(benz)_2(PTA)][PTAH]\cdot EtOH$ (**6**·EtOH). The infrared spectrum of **6** exhibited bands for the PTA ligand at 1025 cm^{-1}, together with $\nu_{Re=O}$ stretching at 945 cm^{-1}. The ^1H NMR spectrum displayed signals for the methylene protons of PTA between 2.91 and 3.29 ppm as well as aromatics between 7.24 and 7.96 ppm. The ^{31}P NMR spectrum showed two singlet peaks for two PTA ligands at −90.4 and −94.5 ppm. The stability of **6** was examined in D_2O via ^{31}P NMR spectroscopy, which

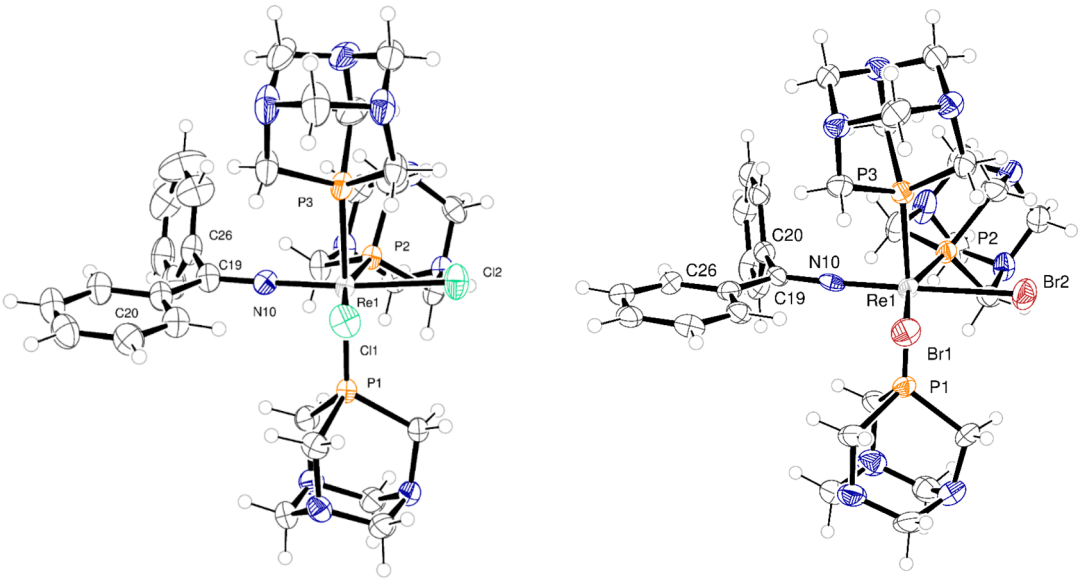

Figure 4. Molecular structures of **4**·2EtOH and **5**·1.6EtOH. Selected bond lengths (Å) and angles (deg): For **4**·2EtOH: Re(1)−Cl(1) 2.4517(7), Re(1)−Cl(2) 2.4608(8), Re(1)−P(1) 2.4095(8), Re(1)−P(2) 2.4009(7), Re(1)−P(3) 2.4310(8), Re(1)−N(10) 1.804(2), N(10)−C(19) 1.300(3); Cl(1)−Re(1)−Cl(2) 85.79(3), P(2)−Re(1)−P(1) 92.46(3), Re(1)−N(10)−C(19) 177.5(2). For **5**: Re(1)−Br(1) 2.5960(9), Re(1)−Br(2) 2.6499(9), Re(1)−P(1) 2.3875(19), Re(1)−P(2) 2.387(2), Re(1)−P(3) 2.3923(19), Re(1)−N(10) 1.801(6), N(10)−C(19) 1.307(9); Br(1)−Re(1)−Br(2) 82.88(3), P(2)−Re(1)−P(1) 95.69(7), Re(1)−N(10)−C(19) 177.4(5).

https://dx.doi.org/10.1021/acs.inorgchem.9b03239
Inorg. Chem. XXXX, XXX, XXX−XXX

revealed two singlets at −88.5 and −91.6 ppm, similar to the signals observed for complex **6** in C_6D_6 albeit with slightly downfield shifts. The complex is completely soluble in benzene and less soluble in water. For example, in 5 mL of D_2O, when 100 mg of **6** was dissolved, after filtration, the remaining undissolved solid weighed 40 mg, i.e., 60 wt % uptake.

Complex **6** was isolated as single crystals from EtOH and examined by X-ray diffraction. The molecular structure is shown in Figure 5 (for an alternative view see Figure S7), with

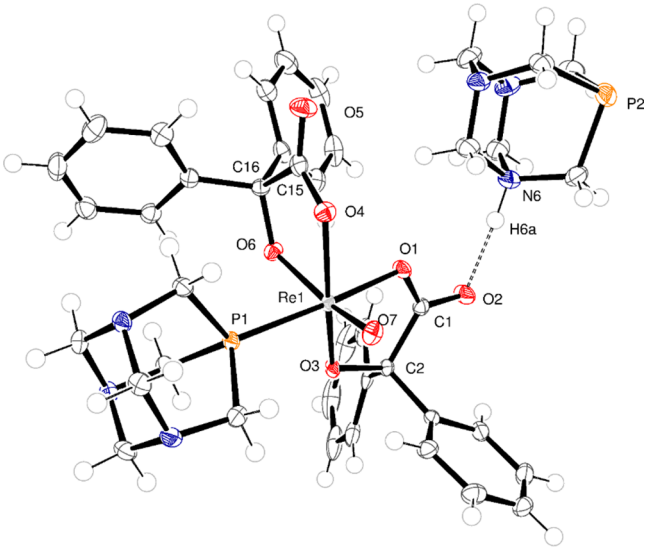

Figure 5. Molecular structure of **6**·EtOH. The dashed line indicates a hydrogen bond. Selected bond lengths (Å) and angles (deg): Re(1)−O(1) 2.0697(14), Re(1)−O(3) 1.9624(14), Re(1)−O(4) 2.1238(14), Re(1)−O(6) 1.9677(14), Re(1)−O(7) 1.7009(15), Re(1)−P(1) 2.3904(5); O(7)-Re(1)-O(1) 97.28(6), O(3)-Re(1)-O(1) 81.02(6), O(6)-Re(1)-O(4) 75.49(6), O(7)-Re(1)-P(1) 89.32(5).

selected bond lengths and angles given in the caption. The rhenium center adopts a distorted octahedral geometry in which the phosphine (Re(1)−P(1) = 2.3904 (5) Å) binds *trans* to the oxygen of an acid group. The main distortion occurs as a result of the chelate binding of the two deprotonated benzilic acid derived ligands. A protonated PTA forms a hydrogen bond with one of the CO benzilic groups. The Re═O bond distance at 1.7009(15) Å is typical.[43] The Re(1)−O(1) bond lengthening of 2.1238(14) Å can be ascribed to the *trans* influence exerted by the Re(1)−P(1).

Potential to Form a Technetium-99m Analogue Compound. In order that the systems herein could be investigated and developed as radiopharmaceuticals, it is necessary (given the 6 h half-life of ^{99m}Tc, used for SPECT imaging) that the product preparation can be conducted from perrhenate in about 4 h. We have chosen perrhenate as the starting material, given the usual source of ^{99m}Tc generated from clinical grade generators in hospital radiopharmacies is pertechnetate.[5] With this in mind, the product [Re(NCPh)(dpg)I(PTA)$_3$] (**7**) was obtained in 4 h by preparing [$ReO_2I(PPh_3)_2$] (from (NH_4)[ReO_4]) and then exchanging the PPh_3 ligands with PTA to afford $ReO_2I(PTA)_3$; then, the $ReO_2I(PTA)_3$ was reacted with two equivalents of $dpgH_2$ in ethanol to afford, after workup, a mixture comprising 85% of complex **7** and 15% of complex **3** (as evidenced by NMR spectroscopy), see Scheme 3.

Scheme 3. One-Pot 4 h Preparation of 3 and 7 from Perrhenate

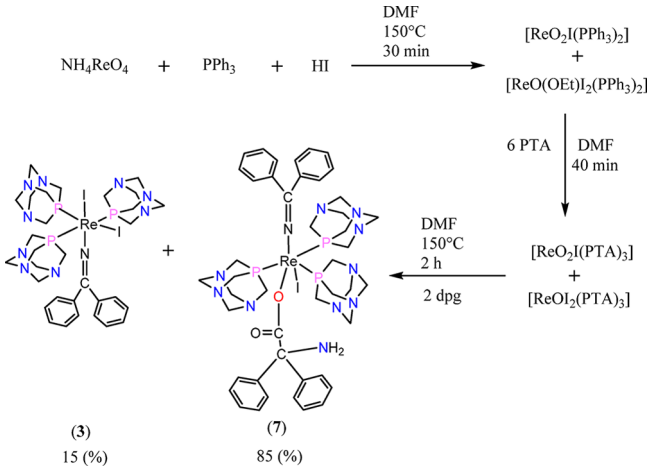

The IR spectrum of **7** exhibited signals associated with PTA ligands in the range of 1012 and 1035 cm^{-1}, together with ν_{Re-O} stretching at 945 cm^{-1} and ν_{NH2} at 3409 cm^{-1}. The ^{1}H NMR spectrum displayed signals for the methylene protons of PTA between 3.55 and 4.34 ppm as well as aromatics between 6.82 and 7.64 ppm. Complex **7** was isolated as single crystals from benzene-d_6 and was examined by X-ray diffraction. The molecular structure is shown in Figure 6 (for an alternative view see Figure S8), with selected bond lengths and angles given in the caption. The rhenium center adopts a distorted octahedral geometry in which the phosphine Re(1)−P(1) binds *trans* to the Re(1)−P(3). One of the dpg ligands has lost CO_2 and binds to the rhenium via the nitrogen atom, in a similar fashion to that observed in **3**. The second diphenylglycine-derived ligand is deprotonated at the carboxylic acid and binds in a monodentate fashion through a single oxygen atom of the carboxylate. Similar to the structure **3**, the Re(1)−P(1) and Re(1)−P(3) bond in a *trans* fashion and display long distances at 2.3932(18) and 2.4017(18) Å, respectively. The Re(1)−I(1) bond lengthening of 2.8101(5) Å can be ascribed to the *trans* influence exerted by Re(1)−P(2) that itself has a bond length 2.3980(16) Å. The Re(1)−O(1) bond lengthening of 2.158(5) Å can also be ascribed to the *trans* influence exerted by Re(1)−N(10) which has a bond length of 1.801(5) Å.

The geometrical parameters associated with the MNCPh$_2$ motif for **3**, **4**, **5**, and **7** are compared in Figure S9. This motif has been called azavinylidene or alkyleneamide,[41] and it is clear there is double bond character associated with the R−N bond. Given the linearity observed here for the Re−N−C angles (>177°), we favor the description put forward by Pombeiro et al.,[41] whereby thus linkage acts as a three electron donor, i.e., as

$$Re \Rightarrow N = CPh_2$$

This then, in terms of electron counting, gives an 18 electron count for the complexes **3**, **4**, **5**, and **7**.

Cell Viability Studies. The complexes **3**, **4**, **5**, **6**, and **7** were tested for cytotoxicity against cancerous cell lines (HeLa, HCT116, and HT-29) to show that they are nontoxic at concentrations used for imaging. The IC_{50} values were determined using the cell viability assay, MTS. All compounds in this study are nontoxic in the concentration range used in

https://dx.doi.org/10.1021/acs.inorgchem.9b03239
Inorg. Chem. XXXX, XXX, XXX−XXX

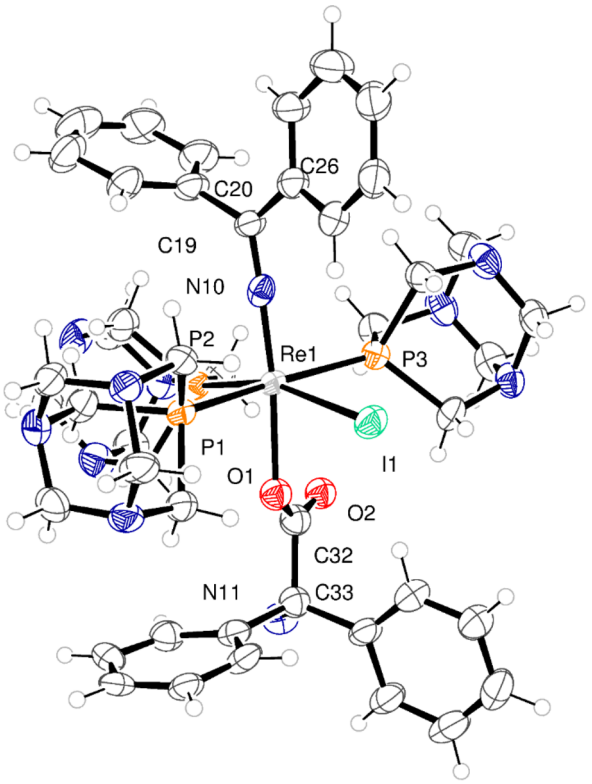

Figure 6. Molecular structure of $7{\cdot}2C_6D_6$. Benzene molecules within the crystal structure are not shown. Selected bond lengths (Å) and angles (deg): Re(1)−O(1) 2.158(5), Re(1)−N(10) 1.801(5), Re(1)−P(1) 2.3932(18), Re(1)−P(2) 2.3980(16), Re(1)−P(3) 2.4017(18), Re(1)−I(1) 2.8101(5), N(10)−C(19) 1.305(8); Re(1)−N(10)−C(19) 177.8(5), N(10)−Re(1)−O(1) 173.3(2), N(10)−Re(1)−P(1) 89.17(16), O(1)−Re(1)−P(1) 84.32(15), N(10)−Re(1)−P(2) 96.65(16).

SPECT medical imaging (nM−pM) with IC_{50} values in the range of 29.87−1858 μM. MTS graphs for treatment of HeLa, HCT116, HT-29, and HEK 293 cells with compounds **3**, **4**, **5**, **6**, and **7** are shown in the Supporting Information, Figures S10−S31. Table 2 summarizes the IC_{50} values of the complexes synthesized.

The analogues compounds **3**, **4**, and **5** show enhanced toxicity in HeLa cells in comparison to that of compounds **6** and **7**, although in colon cancer cell lines (HCT116 and HT-29) compounds **6** and **7** show the higher toxicity (Table 2). When compounds **3**, **6**, and **7** were studied in a noncancerous cell line, there was a dramatic decrease in toxicity to the high micro−millimolar (μM−mM) range, suggesting a preference for antitumor toxicity. The most potent compounds in colon cancer cell lines (**3**, **6**, and **7**) appear to be derived from the iodo starting materials. When looking close at the change of halogen with respect to IC_{50} values, we observed the following trend of I > Br > Cl, which correlates to the size of the halogen and a more labile atom under aqueous environment. The bond distance between the Re metal and the halogen increases with toxicity from 2.86 Å (Re−I), 2.64 Å (Re−Br), and 2.46 Å (Re−Cl), suggesting that the mechanism of action is direct binding of a protein or DNA to the metal center, in a similar manner to that of cisplatin. The IC_{50} values observed here are slightly higher than that of cisplatin for the cancer cell lines (Table 2).[44,45] The addition of the two benzilic acid or diphenylglycine ligands in **6** and **7** with regards to HeLa cells must allow for access to mechanism of resistance in this cell line. Although the mechanism of action has not been explored, it is clear that the change in structure of either amino acid ligands or halogen has an effect on the IC_{50} value. To check the biostability of compound **3** and **7**, a 10 μL sample of compound (6.25 mM) was diluted in 100 μL of biological media (DEME) and monitored by ^{31}P NMR spectroscopy over a period of 5 days; the spectral form does not change across the study (Figures S32−S35). This suggests that the coordination of the water-soluble phosphine ligand (PTA) remains on the metal center and that these are not removed as part of the mechanism of action within the cells. This also suggest that the complexes have a good stability under biological conditions.

Synthesis of Novel Technetium-99m Phosphadamantane Precursor. An attempt was made to translate these protocols to produce technetium-99m analogues of the rhenium complexes. Multistep protocols, such as this, are challenging to translate to radiochemistry where the amounts of the metal ion isotope precursor are limited and the concentrations are low (due to accessible amounts of the radioisotope and radiation protection issues). After several attempts and development of an optimized protocol to produce $[^{99m}Tc][TcO_2I(PPh_3)_2]$ and, subsequently, $[^{99m}Tc]$-$[TcOI_2(PTA)_3]$ from the commercial radioisotope generator supplying $[^{99m}Tc]$pertechnetate, the reaction with diphenylglycine was attempted. Despite the use of various different conditions (including varying temperature, $dpgH_2$ concentration, and time of reaction), the target compound $[^{99m}Tc]$-$[Tc(NCPh_2)I_2(PTA)_3]$ could not be accessed. Further method development is required to produce the technetium analogues from these precursors in an applicable time scale for radiopharmaceutical synthesis.

CONCLUSION

In conclusion, we have used the precursors $[ReOCl_3(PPh_3)_2]$ and $[ReO_2I(PPh_3)_2]$ to access a number of new water-soluble phosphine complexes of rhenium via reaction with 1,2,3-triaza-7-phosphaadamantane (PTA) and the acids diphenylglycine or benzilic acid. Seven complexes have been successfully synthesized and fully characterized, and in a number of cases

Table 2. IC_{50} (μM) Values of Re Complexes Synthesized Herein and of Cisplatin[44−46]

complex	HeLa IC_{50} (μM)	HCT116 IC_{50} (μM)	HT-29 IC_{50} (μM)	HEK 293 IC_{50} (μM)
3	47.17 ± 1.207	40.69 ± 2.584	49.57 ± 5.833	574.7 ± 0.836
4	86.62 ± 1.032	84.47 ± 1.876	88.22 ± 2.491	–
5	71.72 ± 1.415	37.12 ± 2.358	72.04 ± 1.745	–
6	123.60 ± 0.6227	29.87 ± 2.312	37.29 ± 1.699	662.1 ± 1.062
7	140.10 ± 1.045	42.92 ± 2.117	34.38 ± 3.073	1858 ± 1.377
cisplatin	5.45 ± 0.44[44]	8.2 ± 0.14[45]	2.7 ± 0.86[45]	109 ± 12[46]

https://dx.doi.org/10.1021/acs.inorgchem.9b03239
Inorg. Chem. XXXX, XXX, XXX−XXX

(e.g., **3** and **7**), the acid-derived ligand has lost CO_2 during complexation.

Complexes **3**, **4**, **5**, **6**, and **7** have been screened for their antiproliferative activity against various cancer cell lines in order to show a nontoxic behavior at injected doses for SPECT medical imaging. Preliminary studies to form a technetium-99m analogue show that the $[^{99m}Tc][TcOI_2(PTA)_3]$ complex was successfully synthesized; however, the final $dpgH_2$ complex with ^{99m}Tc remains elusive, under the reaction conditions attempted in this study. Further development of routes to the $[^{99m}Tc][TcdpgH_2]$ complexes is required to allow future potential applications in SPECT imaging to be explored. It is a significant advance to have synthesized these novel compounds with the rhenium analogues in a procedure that can be carried out on an appropriate time scale for transfer to radiopharmaceutical production.

■ ASSOCIATED CONTENT

Supporting Information

The Supporting Information is available free of charge at https://pubs.acs.org/doi/10.1021/acs.inorgchem.9b03239.

Crystallography information, including alternative views of **1**−**7**; cell viability studies, including MTS graphs for complexes against HeLa cells and ^{31}P NMR spectra of the complexes; and information on the hot studies, including experimental preparation and characterization analyses (PDF)

Accession Codes

CCDC 1556454, 1583688, and 1894781−1894787 contain the supplementary crystallographic data for this paper. These data can be obtained free of charge via www.ccdc.cam.ac.uk/data_request/cif, or by emailing data_request@ccdc.cam.ac.uk, or by contacting The Cambridge Crystallographic Data Centre, 12 Union Road, Cambridge CB2 1EZ, UK; fax: +44 1223 336033.

■ AUTHOR INFORMATION

Corresponding Authors

Graeme Stasiuk − *Department of Biomedical Sciences, University of Hull, Hull HU6 7RX, U.K.*; orcid.org/0000-0002-0076-2246; Email: g.stasiuk@hull.ac.uk

Carl Redshaw − *Department of Chemistry & Biochemistry, University of Hull, Hull HU6 7RX, U.K.*; orcid.org/0000-0002-2090-1688; Email: C.Redshaw@hull.ac.uk

Authors

Abdullah F. Alshamrani − *Department of Chemistry & Biochemistry and Department of Biomedical Sciences, University of Hull, Hull HU6 7RX, U.K.*

Timothy J. Prior − *Department of Chemistry & Biochemistry, University of Hull, Hull HU6 7RX, U.K.*; orcid.org/0000-0002-7705-2701

Benjamin P. Burke − *Positron Emission Tomography Research Centre, University of Hull, Hull HU6 7RX, U.K.*

David P. Roberts − *Positron Emission Tomography Research Centre, University of Hull, Hull HU6 7RX, U.K.*

Stephen J. Archibald − *Department of Biomedical Sciences and Positron Emission Tomography Research Centre, University of Hull, Hull HU6 7RX, U.K.*; orcid.org/0000-0001-7581-8817

Lee J. Higham − *School of Natural & Environmental Sciences, Newcastle University, Newcastle upon Tyne NE1 7RU, U.K.*

Complete contact information is available at: https://pubs.acs.org/10.1021/acs.inorgchem.9b03239

Notes

The authors declare no competing financial interest.

■ ACKNOWLEDGMENTS

We thank the Saudi Cultural Bureau for its sponsorship (of A.F.A.). C.R. thanks the Whitelaw Frater Cancer Trust for funding. The EPSRC Mass Spectrometry Service Center at Swansea University and the EPSRC National Crystallographic Service at Southampton are thanked for data collection.

■ REFERENCES

(1) (a) Johannsen, B.; Spies, H. Technetium (V) chemistry as relevant to nuclear medicine. In Technetium and Rhenium Their Chemistry and Its Applications. *Top. Curr. Chem.* **1996**, *176*, 77−121. (b) Volkert, W. A.; Jurisson, S. Technetium-99m chelates as radiopharmaceuticals. In Technetium and Rhenium Their Chemistry and Its Applications. *Top. Curr. Chem.* **1996**, *176*, 123−148.

(2) Abram, U.; Alberto, R. Technetium and rhenium: coordination chemistry and nuclear medical applications. *J. Braz. Chem. Soc.* **2006**, *17*, 1486−1500.

(3) Coogan, M. P.; Doyle, R. P.; Valliant, J. F.; Babich, J. W.; Zubieta, J. Single amino acid chelate complexes of the $M(CO)_3^{+2}$ core for correlating fluorescence and radioimaging studies (M= ^{99m}Tc or Re). *J. Labelled Compd. Radiopharm.* **2014**, *57*, 255−261.

(4) Jurisson, S.; Berning, D.; Jia, W.; Ma, D. Coordination compounds in nuclear medicine. *Chem. Rev.* **1993**, *93*, 1137−1156.

(5) Bartholoma, M. D.; Louie, A. S.; Valliant, J. F.; Zubieta, J. Technetium and gallium derived radiopharmaceuticals: comparing and contrasting the chemistry of two important radiometals for the molecular imaging era. *Chem. Rev.* **2010**, *110*, 2903−2920.

(6) (a) Lepareur, N.; Lacoeuille, F.; Bouvry, C.; Hindré, F.; Garcion, E.; Chérel, M.; Noiret, N.; Garin, E.; Knapp, F. F. Rhenium-188 labeled radiopharmaceuticals: current clinical applications in oncology and promising perspectives. *Front. Med.* **2019**, *6*, 32, DOI: 10.3389/fmed.2019.00132. (b) Volkert, W. A.; Hoffman, T. J. Therapeutic radiopharmaceuticals. *Chem. Rev.* **1999**, *99*, 2269−2292.

(7) Dilworth, J. R.; Parrott, S. J. The biomedical chemistry of technetium and rhenium. *Chem. Soc. Rev.* **1998**, *27*, 43−55.

(8) Bartholomä, M.; Valliant, J.; Maresca, K. P.; Babich, J.; Zubieta, J. Single amino acid chelates (SAAC): a strategy for the design of technetium and rhenium radiopharmaceuticals. *Chem. Commun.* **2009**, *48*, 493.

(9) (a) Manning, H. C.; Goebel, T.; Thompson, R. C.; Price, R. R.; Lee, H.; Bornhop, D. J. Targeted molecular imaging agents for cellular-scale bimodal imaging. *Bioconjugate Chem.* **2004**, *15*, 1488−1495. (b) Banerjee, S. R.; Maresca, K. P.; Francesconi, L.; Valliant, J.; Babich, J. W.; Zubieta, J. New directions in the coordination chemistry of ^{99m}Tc: a reflection on technetium core structures and a strategy for new chelate design. *Nucl. Med. Biol.* **2005**, *32*, 1−20. (c) Storr, T.; Thompson, K. H.; Orvig, C. Design of targeting ligands in medicinal inorganic chemistry. *Chem. Soc. Rev.* **2006**, *35*, 534−544. (d) Lee, S.; Chen, X. Dual-modality probes for in vivo molecular imaging. *Mol. Imaging* **2009**, *8*, 87−100. (e) Lee, S.; Xie, J.; Chen, X. Peptide-based probes for targeted molecular imaging. *Biochemistry* **2010**, *49*, 1364−1376. (f) Della Rocca, J.; Liu, D.; Lin, W. Nanoscale metal-organic frameworks for biomedical imaging and drug delivery. *Acc. Chem. Res.* **2011**, *44* (10), 957−968. (g) Hellebust, A.; Richards-Kortum, R. Advances in molecular imaging: targeted optical contrast agents for cancer diagnostics. *Nanomedicine (London, U. K.)* **2012**, *7*, 429−445. (h) Bouziotis, P.; Psimadas, D.; Tsotakos, T.; Stamopoulos, D.; Tsoukalas, C. Radiolabeled iron oxide nanoparticles as dual-modality SPECT/MRI and PET/MRI agents. *Curr. Top. Med. Chem.* **2013**, *12*, 2694−2702. (i) Ghang, Y. J.; Schramm, M. P.; Zhang, F.; Acey, R. A.; David, C. N.; Wilson, E. H.; Wang, Y.; Cheng, Q.;

Hooley, R. J. Selective cavitand-mediated endocytosis of targeted imaging agents into live cells. *J. Am. Chem. Soc.* **2013**, *135*, 7090−7093.

(10) See, for example: (a) Stasiuk, G. J.; Faulkner, S.; Long, N. J. Novel imaging chelates for drug discovery. *Curr. Opin. Pharmacol.* **2012**, *12*, 576−582. (b) Davies, L. H.; Stewart, B.; Harrington, R. W.; Clegg, W.; Higham, L. J. Air-Stable, Highly Fluorescent Primary Phosphanes. *Angew. Chem., Int. Ed.* **2012**, *51*, 4921−4924. (c) Benz, M.; Spingler, B.; Alberto, R.; Braband, H. Toward Organometallic ^{99m}Tc Imaging Agents: Synthesis of Water-Stable 99Tc-NHC Complexes. *J. Am. Chem. Soc.* **2013**, *135*, 17566−17572. (d) Davies, L. H.; Kasten, B. B.; Benny, P. D.; Arrowsmith, R. L.; Ge, H.; Pascu, S. I.; Botchway, S. W.; Clegg, W.; Harrington, R. W.; Higham, L. J. Re and 99m Tc complexes of BodP 3-multi-modality imaging probes. *Chem. Commun.* **2014**, *50*, 15503−15505. (e) Hahn, E. M.; Casini, A.; Kuehn, F. E. Re (VII) and Tc (VII) trioxo complexes stabilized by tridentate ligands and their potential use as radiopharmaceuticals. *Coord. Chem. Rev.* **2014**, *276*, 97−111. (f) Stasiuk, G. J.; Holloway, P. M.; Rivas, C.; Trigg, W.; Luthra, S. K.; Morisson Iveson, V.; Gavins, F. N. E.; Long, N. J. 99m Tc SPECT imaging agent based on cFLFLFK for the detection of FPR1 in inflammation. *Dalton Trans* **2015**, *44*, 4986−4993. (g) Amoroso, A. J.; Fallis, I. A.; Pope, S. J. Chelating agents for radiolanthanides: Applications to imaging and therapy. *Coord. Chem. Rev.* **2017**, *340*, 198−219. (h) Mishiro, K.; Hanaoka, H.; Yamaguchi, A.; Ogawa, K. Radiotheranostics with radiolanthanides: Design, development strategies, and medical applications. *Coord. Chem. Rev.* **2019**, *383*, 104−131.

(11) Fernández-Moreira, V.; Ortego, M. L.; Williams, C. F.; Coogan, M. P.; Villacampa, M. D.; Gimeno, M. C. Bioconjugated rhenium (I) complexes with amino acid derivatives: synthesis, photophysical properties, and cell imaging studies. *Organometallics* **2012**, *31*, 5950−5957.

(12) Ferná'ndez-Moreira, V.; Thorp-Greenwood, F. L.; Amoroso, A. J.; Cable, J.; Court, J. B.; Gray, V.; Hayes, A. J.; Jenkins, R. L.; Kariuki, B. M.; Lloyd, D.; Millet, C. O.; Williams, C. F.; Coogan, M. P. Uptake and localisation of rhenium fac-tricarbonyl polypyridyls in fluorescent cell imaging experiments. *Org. Biomol. Chem.* **2010**, *8*, 3888−3901.

(13) Nayak, D. K.; Halder, K. K.; Baishya, R.; Sen, T.; Mitra, P.; Debnath, M. C. Tricarbonyltechnetium (I) and tricarbonylrhenium (I) complexes of amino acids: Crystal and molecular structure of a novel cyclic dimeric $Re(CO)_3$-amino acid complex comprised of the OON donor atom set of the tridentate ligand. *Dalton Trans.* **2013**, *42*, 13565−13575.

(14) Tubis, M.; Endow, J. S. The preparation of 99mTechnetium-labeled cystine, methionine and a synthetic polypeptide and their distribution in mice. *Int. J. Appl. Radiat. Isot.* **1968**, *19*, 835−840.

(15) Maresca, K. P.; Marquis, J. C.; Hillier, S. M.; Lu, G.; Femia, F. J.; Zimmerman, C. N.; Eckelman, W. C.; Joyal, J. L.; Babich, J. W. Novel polar single amino acid chelates for technetium-99m tricarbonyl-based radiopharmaceuticals with enhanced renal clearance: application to octreotide. *Bioconjugate Chem.* **2010**, *21*, 1032−1042.

(16) King, R.; Surfraz, M. B. U.; Finucane, C.; Biagini, S. C.; Blower, P. J.; Mather, S. J. 99mTc-HYNIC-gastrin peptides: assisted coordination of ^{99m}Tc by amino acid side chains results in improved performance both in vitro and in vivo. *J. Nucl. Med.* **2009**, *50*, 591−598.

(17) Sparr, C.; Michel, U.; Marti, R. E.; Müller, C.; Schibli, R.; Moser, R.; Groehn, V. Synthesis of a Novel γ-Folic Acid-Nτ-Histidine Conjugate Suitable for Labeling with 99mTc and 188Re. *Synthesis* **2009**, *2009*, 787−792.

(18) Law, G.-L.; Kwok, W.-M.; Wong, W.-T.; Wong, K.-L.; Tanner, P. A. Terbium Luminescence Sensitized through Three-Photon Excitation in a Self-Assembled Unlinked Antenna. *J. Phys. Chem. B* **2007**, *111*, 10858−10861.

(19) Law, G.-L.; Wong, K.-L.; Lau, K.-K.; lap, S. -t.; Tanner, P. A.; Kuo, F.; Wong, W.-T. Nonlinear optical activity in dipolar organic-lanthanide complexes. *J. Mater. Chem.* **2010**, *20*, 4074−4079.

(20) (a) Braun, M. The"“ ""magic"“" diarylhydroxymethyl group. *Angew. Chem.* **1996**, *108*, 565−568; *Angew. Chem., Int. Ed. Engl.* **1996**, *35*, 519−522. (b) Braun, M. The diaryl (oxy) methyl group: More than an innocent bystander in chiral auxiliaries, catalysts, and dopants. *Angew. Chem., Int. Ed.* **2012**, *51*, 2550−2562.

(21) Al-Khafaji, Y. F.; Elsegood, M. R. J.; Frese, J. W.; Redshaw, C. Ring opening polymerization of lactides and lactones by multimetallic alkyl zinc complexes derived from the acids $Ph_2C(X)CO_2H$ (X= OH, NH_2). *RSC Adv.* **2017**, *7*, 4510−4517.

(22) Al-Khafaji, Y. F.; Prior, T. J.; Horsburgh, L.; Elsegood, M. R. J.; Redshaw, C. Multimetallic Lithium Complexes Derived from the Acids $Ph_2C(X)CO_2H$ (X= OH, NH_2): Synthesis, Structure and Ring Opening Polymerization of Lactides and Lactones. *Chem. Select.* **2017**, *2*, 759−768.

(23) (a) Redshaw, C.; Elsegood, M. R. J.; Holmes, K. E. Synthesis of Hexa-and Dodecanuclear Organoaluminum Ring Structures Incorporating the"“ ""Magic"“" Ph_2C (X) Group (X= O-, NH-). *Angew. Chem., Int. Ed.* **2005**, *44*, 1850−1853. (b) Redshaw, C.; Elsegood, M. R. J. Synthesis of Tetra-, Hexa-, and Octanuclear Organozinc Ring Systems. *Angew. Chem., Int. Ed.* **2007**, *46*, 7453−7457.

(24) Marchi, A.; Marchesi, E.; Marvelli, L.; Bergamini, P.; Bertolasi, V.; Ferretti, V. New Water-Soluble Rhenium Complexes with 1, 3, 5-Triaza-7-phosphaadamantane (PTA)-X-ray Crystal Structures of $[ReNCl_2(PTA)_3]$,$[ReO_2Cl(PTA)_3]$,$[ReCl_3(PTA)_2(PPh_3)]$, and $[Re_2N_2Cl_3(Et_2\ dtc)(PTA)_4]$. *Eur. J. Inorg. Chem.* **2008**, *2008* (17), 2670−2679.

(25) Daigle, D. J.; Pepperman, A. B., Jr; Vail, S. L. Synthesis of a monophosphorus analog of hexamethylenetetramine. *J. Heterocycl. Chem.* **1974**, *11* (3), 407−408.

(26) Daigle, D. J.; Decuir, T. J.; Robertson, J. B.; Darensbourg, D. J. 1,3,5-Triaz-7-Phosphatricyclo [3.3. 1.13, 7] Decane and Derivatives. *Inorg. Synth.* **2007**, *32*, 40−45.

(27) Martins, L. M.; Alegria, E. C.; Smoleński, P.; Kuznetsov, M. L.; Pombeiro, A. J. Oxorhenium Complexes Bearing the Water-Soluble Tris (pyrazol-1-yl) methanesulfonate, 1,3,5-Triaza-7-phosphaadamantane, or Related Ligands, as Catalysts for Baeyer-Villiger Oxidation of Ketones. *Inorg. Chem.* **2013**, *52*, 4534−4546.

(28) Bravo, J.; Bolaño, S.; Gonsalvi, L.; Peruzzini, M. Coordination chemistry of 1,3,5-triaza-7-phosphaadamantane (PTA) and derivatives. Part II. The quest for tailored ligands, complexes and related applications. *Coord. Chem. Rev.* **2010**, *254*, 555−607.

(29) Phillips, A. D.; Gonsalvi, L.; Romerosa, A.; Vizza, F.; Peruzzini, M. Coordination chemistry of 1,3,5-triaza-7-phosphaadamantane (PTA): transition metal complexes and related catalytic, medicinal and photoluminescent applications. *Coord. Chem. Rev.* **2004**, *248*, 955−993.

(30) Guerriero, A.; Peruzzini, M.; Gonsalvi, L. Coordination chemistry of 1,3,5-triaza-7-phosphatricyclo [3.3. 1.1] decane (PTA) and derivatives. Part III. Variations on a theme: Novel architectures, materials and applications. *Coord. Chem. Rev.* **2018**, *355*, 328−361.

(31) (a) Herrmann, W. A.; Kusthardt, U.; Ziegler, M. L.; Zahn, T. Novel C-O Bond Formation via [3 + 2] Cycloaddition of Diphenylketene to a Dioxo Metal Moiety. *Angew. Chem., Int. Ed. Engl.* **1985**, *24*, 860. (b) Herrmann, W. A.; Roesky, P. W.; Scherer, W.; Kleine, M. Multiple bonds between main-group elements and transition metals, 140. Cycloaddition reactions of methyltrioxorhenium (VII): diphenylketene and sulfur dioxide. *Organometallics* **1994**, *13*, 4536. (c) Middleditch, M.; Anderson, J. C.; Blake, A. J.; Wilson, C. A series of [3+ 2] Cycloaddition products from the reaction of rhenium oxo complexes with diphenyl ketene. *Inorg. Chem.* **2007**, *46*, 2797−2804.

(32) Rouschias, G.; Wilkinson, G. The preparation and reactions of trihaolgeno (alkanonitrile) bis (triphenylphosphine) rhenium (III) complexes. *J. Chem. Soc. A* **1967**, 993−1000.

(33) Chatt, J.; Rowe, G. A. Complex compounds of tertiary phosphines and a tertiary arsine with rhenium (V), rhenium (III), and rhenium (II). *J. Chem. Soc.* **1962**, 4019−4033.

(34) Ciani, G. F.; D'Alfonso, G.; Romiti, P. F.; Sironi, A.; Freni, M. Rhenium (V) oxide complexes. Crystal and molecular structures of

https://dx.doi.org/10.1021/acs.inorgchem.9b03239
Inorg. Chem. XXXX, XXX, XXX−XXX

the compounds trans-$ReI_2O(OR)(PPh_3)_2$ (R = = Et, Me) and of their hydrolysis derivative $ReIO_2(PPh_3)_2$. *Inorg. Chim. Acta* **1983**, *72*, 29−37.
(35) Blessing, R. H. An empirical correction for absorption anisotropy. *Acta Crystallogr., Sect. A: Found. Crystallogr.* **1995**, *A51*, 33−38.
(36) Sheldrick, G. M. Integrated space-group and crystal structure determination. *Acta Crystallogr., Sect. A: Found. Adv.* **2015**, *A71*, 3−8.
(37) Sheldrick, G. M. Crystal structure refinement with SHELXL. *Acta Crystallogr., Sect. C: Struct. Chem.* **2015**, *71*, 3.
(38) Rouschias, G. Recent advances in the chemistry of rhenium. *Chem. Rev.* **1974**, *74*, 531−566.
(39) Gibson, V. C.; Redshaw, C.; Clegg, W.; Elsegood, M. R. J. Synthesis and characterisation of molybdenum complexes bearing highly functionalised imido substituents. *J. Chem. Soc., Dalton Trans.* **1997**, 3207−3212.
(40) Wang, X.; Zhao, K. Q.; Al-Khafaji, Y.; Mo, S.; Prior, T. J.; Elsegood, M. R. J.; Redshaw, C. Organoaluminium Complexes Derived from Anilines or Schiff Bases for the Ring-Opening Polymerization of ε-Caprolactone, δ-Valerolactone and rac-Lactide. *Eur. J. Inorg. Chem.* **2017**, *2017*, 1951−1965.
(41) (a) Erker, G.; Frömberg, W.; Atwood, J. L.; Hunter, W. E. Hydrozirconation of Nitriles: Proof of a Linear Heteroallene Structure in (Benzylideneamido) zirconocene Chloride. *Angew. Chem.* **1984**, *96*, 72−73; *Angew. Chem., Int. Ed. Engl.* **1984**, *23*, 68−69. (b) Frömberg, W.; Erker, G. Hydrozirconierung von nitrilen: Die bildung ein-und zweikerniger (alkylidenamido) zirconocen-komplexe. *J. Organomet. Chem.* **1985**, *280*, 343−354. (c) Werner, H.; Knaup, W.; Dziallas, M. A Novel Route to Azaalkenylidene-Metal Complexes. *Angew. Chem., Int. Ed. Engl.* **1987**, *26*, 248−250. (d) Pombeiro, A. J.; Hughes, D. L.; Richards, R. L. A novel route to methyleneamido ligands by protonation of nitriles ligating an electron-rich center. Synthesis of trans-$[ReCl(NCR)(dppe)_2]$(R= alkyl or aryl, dppe= $Ph_2PCH_2CH_2PPh_2$) and $[ReCl(N{=}CHC_6H_4OMe\text{-}4)(dppe)_2][BF_4]$. *J. Chem. Soc., Chem. Commun.* **1988**, 1052−1053. (e) Frá'usto da Silva, J. J.R.; C. Guedes da Silva, M.F.; Henderson, R. A.; Pombeiro, A. J.L.; Richards, R. L. Protonation of the nitrite ligand versus protonation of rhenium at cis-or trans-$[ReCl(NCC_6H_4R\text{-}4)(Ph_2PCH_2CH_2PPh_2)_2]$(R Cl, F, Me or MeO). A mechanistic study. *J. Organomet. Chem.* **1993**, *461*, 141−145. (f) Brown, S. N. Oxidative azavinylidene formation in the reaction of 1, 3-diphenylisobenzofuran with osmium nitride complexes. *Inorg. Chem.* **2000**, *39*, 378−381. (g) Tanabe, Y.; Seino, H.; Ishii, Y.; Hidai, M. Reaction Mechanism of the C: N Triple Bond Cleavage of β-Ketonitriles on a Molybdenum (0) Center1. *J. Am. Chem. Soc.* **2000**, *122*, 1690−1699. (h) Castarlenas, R.; Esteruelas, M. A.; Gutiérrez-Puebla, E.; Jean, Y.; Lledós, A.; Martín, M.; Oñate, E.; Tomàs, J. Synthesis, Characterization, and Theoretical Study of Stable Hydride- Azavinylidene Osmium (IV) Complexes. *Organometallics* **2000**, *19*, 3100−3108. (i) Castarlenas, R.; Esteruelas, M. A.; Gutiérrez-Puebla, E.; Oñate, E. Reactivity of the Imine- Vinylidene Complexes $OsCl_2(C = C{=}HPh)(NH\ CR_2)(PiPr_3)_2$ $[CR_{2=}\ CMe_2,\ C(CH_2)\ 4CH_2]$. *Organometallics* **2001**, *20*, 1545−1554. (j) Castarlenas, R.; Esteruelas, M. A.; Oñate, E. One-Pot Synthesis for Osmium (II) Azavinylidene- Carbyne and Azavinylidene- Alkenylcarbyne Complexes Starting from an Osmium (II) Hydride- Azavinylidene Compound. *Organometallics* **2001**, *20*, 3283−3292. (k) Castarlenas, R.; Esteruelas, M. A.; Jean, Y.; Lledós, A.; Oñate, E.; Tomàs, J. Formation and Stereochemistry of Octahedral Cationic Hydride-Azavinylidene Osmium (IV) Complexes. *Eur. J. Inorg. Chem.* **2001**, *2001*, 2871−2883. (l) Guedes da Silva, M. F. C.; Fraústo da Silva, J. J.; Pombeiro, A. J. Activation of Organonitriles toward β-Electrophilic Attack. Synthesis and Characterization of Methyleneamide (Azavinylidene) Complexes of Rhenium. *Inorg. Chem.* **2002**, *41*, 219−228. (m) Ugolotti, J.; Kehr, G.; Fröhlich, R.; Grimme, S.; Erker, G. Nitrile insertion into a boryl-substituted five-membered zirconacycloallenoid: unexpected formation of a zwitterionic boratirane product. *Chem. Commun.* **2009**, 6572−6573. (n) Podiyanachari, S. K.; Fröhlich, R.; Daniliuc, C. G.; Petersen, J. L.; Mück-Lichtenfeld, C.; Kehr, G.; Erker, G. Hydrogen Activation by an Intramolecular Boron Lewis Acid/Zirconocene Pair. *Angew. Chem., Int. Ed.* **2012**, *51*, 8830−8833; *Angew. Chem.* **2012**, *124*, 8960−8963. (o) Lu, E.; Zhou, Q.; Li, Y.; Chu, J.; Chen, Y.; Leng, X.; Sun, J. Reactivity of scandium terminal imido complexes towards metal halides. *Chem. Commun.* **2012**, *48*, 3403−3405. (p) Huang, J. S.; Wong, K. M.; Chan, S. L. F.; Tso, K. C. H.; Jiang, T.; Che, C. M. Ketimido Metallophthalocyanines: An Approach to Phthalocyanine-Supported Mononuclear High-Valent Ruthenium Complexes. *Chem. - Asian J.* **2014**, *9*, 338−350. (q) Chen, J.; Huang, Z. A.; Lu, Z.; Zhang, H.; Xia, H. Synthesis of Cyclic Vinylidene Complexes and Azavinylidene Complexes by Formal [4+ 2] Cyclization Reactions. *Chem. - Eur. J.* **2016**, *22*, 5363−5375.
(42) Allen, F. H. The Cambridge Structural Database: a quarter of a million crystal structures and rising. *Acta Crystallogr., Sect. B: Struct. Sci.* **2002**, *58*, 380−388.
(43) See, for example: (a) Iengo, E.; Zangrando, E.; Mestroni, S.; Fronzoni, G.; Stener, M.; Alessio, E. Complexed bridging ligands: oxorhenium (V) compounds with mono-coordinated pyrazine or pyrimidine as possible building blocks for the construction of polynuclear architectures. *J. Chem. Soc., Dalton Trans.* **2001**, 1338−1346. (b) Redshaw, C.; Liu, X.; Zhan, S.; Hughes, D. L.; Baillie-Johnson, H.; Elsegood, M. R. J.; Dale, S. H. Rhenium calix[4]arenes: Precursors to novel imaging and cancer therapy agents. *Eur. J. Inorg. Chem.* **2008**, *2008*, 2698−2712.
(44) Wahab, A.; Ibrahim, S.; Abdul, A. B.; Alzubairi, A. S.; Elhassan, M. M.; Mohan, S. In vitro ultramorphological assessment of apoptosis induced by zerumbone on (HeLa). *Int. J. Pharmacol.* **2009**, *5*, 71−75.
(45) Poindessous, V.; Koeppel, F.; Raymond, E.; Cvitkovic, E.; Waters, S. J.; Larsen, A. K. Enhanced antitumor activity of irofulven in combination with 5-fluorouracil and cisplatin in human colon and ovarian carcinoma cells. *Int. J. Oncol.* **2003**, *23*, 1347−1355.
(46) Suntharalingam, K.; Hunt, D. J.; Duarte, A. A.; White, A. J.; Mann, D. J.; Vilar, R. A Tri-copper (II) Complex Displaying DNA-Cleaving Properties and Antiproliferative Activity against Cancer Cells. *Chem. - Eur. J.* **2012**, *18*, 15133−15141.

https://dx.doi.org/10.1021/acs.inorgchem.9b03239
Inorg. Chem. XXXX, XXX, XXX−XXX